https://doi.org/10.1016/j.conbuildmat.2015.10.021

Construction and Building Materials

A study on the relationship between Mean Texture Depth and Mean Profile Depth of asphalt pavements

F.G. Praticò[a] *and* **R. Vaiana**[b]

[a] DIIES Department, University Mediterranea of Reggio Calabria, via Graziella Feo di Vito, Italy Tel/fax +39 0965 875230 – 875471 e-mail: filippo.pratico@unirc.it

[b] Department of Civil Engineering, University of Calabria, Arcavacata Campus of Rende, Cosenza, Italy, tel/fax +39 0984 496786, e-mail vaiana@unical.it

Keywords: pavement macrotexture; MPD mean profile depth; MTD mean texture depth; laser profilometer.

Abstract

Safety, skid resistance and noise of roads highly depend on the characteristics of pavement surface texture, for both porous and dense-graded wearing courses.

In the light of the above facts, the objective of the study was to model the relationship between laser-based and volumetric-type measurements of the surface macro-texture of a pavement. In more detail, the study focused on the mean profile depth (MPD, as *per* ISO 13473-1 [1] and ASTM E 1845 [2]) and on the mean texture depth (MTD, as known as sand patch texture, as *per* ASTM E 965 [3] and EN 13036-1 [4]). Different types of surface textures were considered: dense-graded friction courses (DGFC), spittmastic asphalts (SMA), open-graded friction courses (OGFC), porous European mixes (PEM).

A generalized simple model has been set up, calibrated and validated. The proposed model fits the data of many types of wearing courses without neglecting the basic achievements which refer to the curves previously derived.

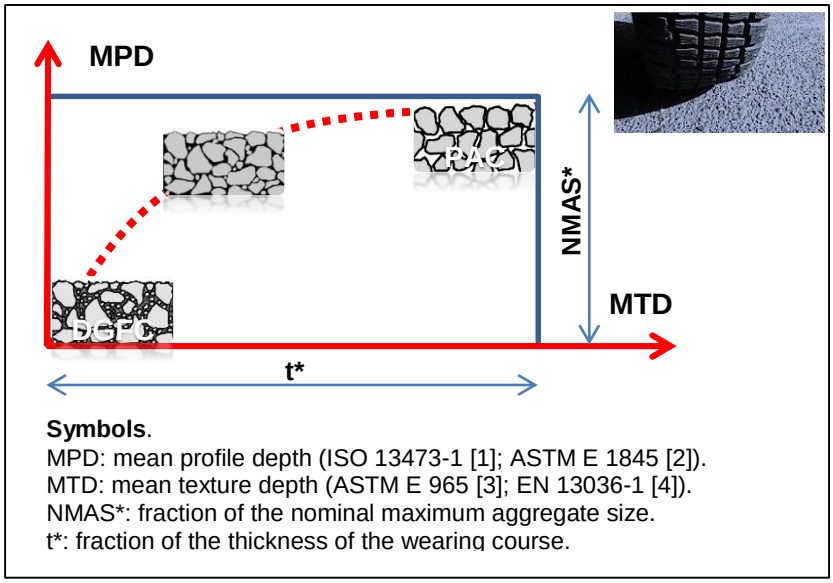

Graphical abstract

1.Background

Surface texture has an outstanding importance in terms of road and airport safety (Noyce et al, 2005 [5]). It affects as well pavement performance (Freitas et Al., 2008 [6]): i) tyre/road friction, (NCHRP 291, 2000 [7]; Do et Al., 2004 [8]; Kim et al, 2013 [9]); ii) noise emission (SILVIA, 2006 [10]; Lu and Harvey, 2011 [11]; Praticò et al., 2013 [12]; Praticò et al., 2014 [13]) driving comfort (Delanne and Daburon, 1999 [14]); iii) rolling resistance (Bendtsen 2004 [15]; Sohaney and Rasmussen, 2013 [16]); iv) wear of tyres (Nordströdm and Andersson, 1996 [17]; Domenichini and Martinelli, 2004 [18]); v) particulate matter emission from paved roads (China and James, 2012 [19]; Amato et al., 2013 [20]); vi) operating costs (Bendtsen, 2004 [15]); vii) greenhouse gas emissions. (Wang et al, 2014 [21]) focused on macrotexture (MPD, MTD) impact on life cycle GHG (greenhouse gas) emissions. Indeed, macrotexture refers to the primary wavelengths that excite shock absorbers in vehicle suspension systems, cause deformation of tire sidewalls for a moving vehicle, affect energy dissipation, waste heat, and rolling resistance by vehicles.

Surface macrotexture (wavelengths between 0.5 and 50mm) can be assessed through intrinsic and extrinsic indicators (Boscaino and Pratico, 2001 [22]). In more detail, the following main methods apply: volumetric methods (ASTM E965 [3] procedure, with glass spheres; EN 13036-1 [4], with glass spheres), laser-based methods (ASTM E 1845 [2]; ISO 13473-1 [1]; Abe et Al., 2001 [23]; Aktaş et Al., 2011 [24]; Blanchard and Holloway, 2013 [25]; China and James, 2012 [26]; Sengoz et al., 2012 [27]), and permeability-related methods (ASTM STP 583 [28], Cooley, 1999 [29]). Note that volumetric methods and indicators (e.g., MTD) are based on the ratio between a volume and a surface area, while laser-based methods and indicators (e.g., MPD) rely on the ratio between a surface area and a length. (Yaacob et al, 2014 [30]) assessed pavement texture with variety of test methods, including sand patch test and multi laser profiler. They concluded that there were weak correlations between the results of these two measurement techniques. (Rodriguez et al., 2014 [31]) advised the use of 3D texturometer laser, as a method of measuring the surface macrotexture and MPD (Mean Profile Depth) in order to estimate indicators derived by Sand and Grease Patch tests. Surface texture depends on mix components and construction process (Stroup-Gardiner and Brown, 2000 [32]; Davis, 2001 [33]; Flintsch et al, 2003 [34]; Hanson and Prowell, 2004 [35]; Sullivan, 2005 [36]; Goodman et al, 2006 [37]; Praticò et al, 2010 [38]; D'apuzzo et al, 2012 [39]).

The sand patch method (see ASTM E 965 [3], EN 13036-1 [4] and previous standards in which sand was used instead of glass spheres) is suitable for bituminous surface courses and concrete pavement surfaces with texture depth greater than about 0.25 mm and is affected by the surface and inner structure of the mixture (air voids distribution, shape, tortuosity). Sand patch method depends on dense granular (glass beads) flows. It is size-dependent and a complicated set of flow properties are involved, which differentiate them from ordinary fluids (Henann and Kamrin, 2013 [40]) .

Laser-type measurements (see ASTM E 1845 [2] and ISO 13473-1 [1]) are affected by the complex shape of a pavement surface but they do not depend on what the laser cannot "see" from its position. In more detail, even when conoscopic holography is used (which presents several advantages), a laser beam is projected onto the surface and then the immediate reflection along the same ray-path are put through a conoscopic crystal and projected onto a CCD (charge-coupled device for the movement of electrical charge). The result is a diffraction pattern. This pattern is frequency analysed and the distance to the measured surface (pavement surface) is consequently derived. The main advantage with conoscopic holography is that only a single ray-path is needed for measuring, thus giving an opportunity to measure very deep pavement "valleys". Criticalities (as

for all the laser-based techniques) relate to beam dimensions and to the fact that beams describe a family of straight lines, without any possibility to investigate pores properties outside the above plane.

Accurate sand patch testing on/and laser based testing cannot be carried out when road surface is sticky or wet. The equipment of the sand patch method costs around 0.1k€ while the equipment of a laser-based texture equipment costs around 10-100k€. The duration of the two tests ranges from less than one second (high-speed laser measurement), to a couple of minutes (sand patch method), to several minutes (high-precision, laboratory-type lasers).
Pavement Macrotexture Depth (herein termed MTD, ASTM E 965 [3], EN 13036-1 [4]) and Mean profile depth (MPD, ASTM E 1845 [2] and ISO 13473-1 [1]) are indicators which refer to macrotexture domain (wavelengths between 0.5 and 50 mm). Two main domains can be approximately observed with reference to macrotexture studies and analyses (Meegoda et al, 2002 [41]): low macrotextures (MPD lower than about 1.5 mm) and high macrotextures (MPD higher than about 1.5mm).

In the first dominion many linear relationships MTD(MPD) have been derived. The slope of the equation used to obtain MTD from MPD measurements takes values from about 0.5 to 1.2. In particular, values of 0.5-0.6 were found by (Vaiana et al, 2012 [42]; Kim et al, 2013 [9]), whereas (Freitas et al, 2008 [6]) found a slope value of 0.7. According to (Wambold et al, 1995 [43]; ASTM E-1845 [2]; ISO 13473-1 [1]; Wang et al, 2011 [44]; Losa et al, 2007 [45]; De Fortier and Waller, 2007 [46]; Mackey 2005 [47]; Flintsch et al, 2007 [48]) the range of slope was 0.8-1. Finally, Sengoz et al. 2012 [27] and Fisco and Sezen, 2013 [49] found slope values of 1.1 and 1.2, respectively.

The intercepts range from about -0.3 (Flintsch et al, 2002 [50]), to 0.0 (Hanson and Prowell, 2004 [35]), to 0.2 (Wambold et al, 1995 [43]; ASTM E-1845 [2]; ISO 13473-1 [1]; Wang et al, 2011 [44]; Vaiana et al, 2012 [42]), to 0.3 (Kim et al, 2013 [9]), to 1 (Xiao et al, 2011 [51], MPD based on miscroscopy evaluation).

It is noted that several lasers, due to their characteristics, yield other linear relationship (ASTM E2157-2005 [52]). For example, for the CTMeter, the slope is about 0.95 and the intercepts is about 0.07 (Fisco and Sezen, 2013 [49]).

In the second dominion (higher values of macrotexture) many authors have found results which do not comply with the previous equations (e.g., Hanson and Prowell, 2004 [35]).
According to ISO 13473-1 [1], experience has shown that the sand patch texture may be not reliable if used in porous surfaces because some material may pour down into the pores (Freitas et al, 2008 [6]).

According to (Noyce et al, 2005 [5]), the prediction of MTD (mean texture depth, volumetric method) from MPD (Mean profile depth, ASTM E 1845 [2]) is not valid for highly porous surfaces, as the glass spheres or sand flows into the pores, producing high values for MTD. Furthermore, at the same time, (Noyce et al, 2005 [5]) found that the prediction of OFT (ASTM STP 583 [28], outflow time) from MTD was very good also for highly porous surfaces. Note that the existence of a different relationship between MPD and MTD for porous asphalt concretes (PAC) or similar surfaces (open-graded friction courses, OGFC, porous European mixes, PEM; etc.) has been pointed out by many other authors (Other data. Hanson and Prowell, 2004 [35]; Nicholls 1997 [53], Hanson and Prowell, 2004 [35]; Flintsch et al, 2002 [50]).

(Vilaça et al, 2010 [54]) developed a scanning prototype to derive ETD and results obtained showed a certain difference between the predicted and the actual value of texture for “rough” porous asphalt concretes.

(Praticò and Vaiana, 2013 [55]) studied the variability of MPD-related and ETD-related measurements for porous asphalt concrete. Their standard deviation and coefficient of variation resulted comparable.

Note that when comparing CTMeter and sand patch method, (Hanson and Prowell, 2004 [35]; Prowell and Hanson, 2005 [56]) found that the offset between the CTMeter and sand patch test results was insignificant when open-graded mixtures were excluded.

(Freitas et al, 2014 [57]) focused on the variability of the mean profile depth and pointed out the necessity to further investigate the effect of the type of surface on data variability.
Finally, note that the inherent proportionality between MPD and the NMAS (nominal maximum aggregate size) has been partly proved by (Henault et al., 2011 [58]). In contrast, this fact didn’t happen when comparing MTD and NMAS. Note that Superpave defines NMAS as “one sieve size larger than the first sieve to retain more than 10 percent of the material” (Roberts et al., 1996 [59]).

2.Objectives

Safety, skid resistance and noise of roads highly depend on the characteristics of pavement texture, for both porous and dense-graded wearing courses.

Consequently, there is a strong need to develop methods and algorithms to quickly estimate the characteristics of road surface textures, without traffic interruptions, over a wider range of pavement types. To this end, assessing relationships which are valid for different types of friction courses can have an appreciable impact, in a context in which porous asphalt concretes and other innovative wearing courses are widely used.

In the light of the above facts, the objective of the study was to model the relationship between laser-based and volumetric-type measurements of the surface macro-texture of a pavement. In more detail, the study focused on the mean profile depth (ISO 13473-1 [1] and ASTM E 1845 [2]) and on the mean texture depth (ASTM E 965 [3] and EN 13036-1 [4]). Different types of surface textures were considered: dense-graded friction courses (DGFC), spittmastic asphalts (SMA), open-graded friction courses (OGFC), porous European mixes (PEM). Modelling was followed by calibration and validation.

The remaining part of the paper is organised into section 3, in which the model building, calibration and validation is described, and section 4, in which conclusion are drawn.

3. Model and experimental validation

The methodology for building and validating the model is below summarized in terms of three main tasks.

Task 1. Model building. During this phase the model was set up, based on literature study and analysis (see above), data analysis, modelling of the boundary conditions (conditions in extreme points of the range of variation of the two main variables (MTD, MPD).

Task 2. Model calibration. In order to check whether the model fits experimental measurements or other empirical data, these latter were split into two disjoint subsets: training data and verification

data. Many types of surface courses were considered for the dataset building (see Table 1): two Stone Mastic Asphalts (S1 and S2); two Porous European Mixes (P1 and P2); a porous asphalt concrete (P3) for which data were derived from a literature review; a dense graded friction course (D1), see table 1.

Task 3. Model verification. The verification data were derived from an experimental plan, *ad hoc* designed and carried out. In this case, a Porous European Mix (P4) and a Dense Graded Friction Course (D2) were considered.

3.1 Model building

The set of data used for analysis and calibration is shown in Figure 1. In the same picture the equality line (solid line) and the PIARC 1995 equation (dotted line, Wambold et al. 1995 [43]) are represented.

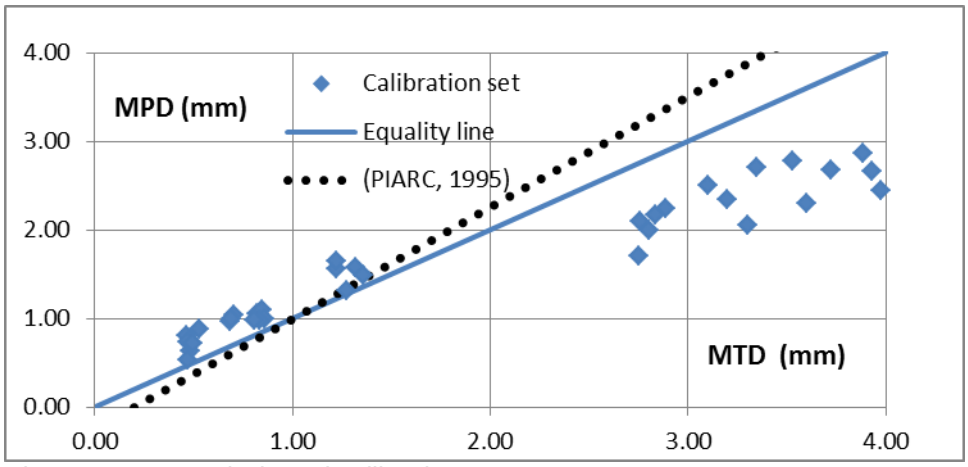

Figure 1. Data analysis and calibration

It is possible to observe what follows.

In the range below about 1.5 mm, a linear equation seems to represent well the data. As is well known, the intercept around 0.2mm (dotted line, Wambold et al. 1995 [43]) can be associated to the diameter of the spheres (beads or sand) when the surface tends to be flat.

In other terms, in the case of very dense surfaces, the lowest MTD is associated with a cylinder 0.2mm –thick. In turn, in the case of very dense surfaces, MPD tends to a minimum value which is zero, being based on a laser measurement of differences from the peak, as per the EN standard.

In the range above about 1.5mm, there is a clear divergence of data from the abovementioned linear relationships which refer to low macrotexture domain.

Higher MPDs yield higher MTD, but the slope MTD/MPD (the change in MTD divided by the change in MPD) varies and tends to increase (MTD>>MPD). *Vice versa*, the slope MPD/MTD (see Figure 1 tends to decrease and to reach a value close to zero.

On average, considering only data above 1.5mm, the slope is about one fourth of the slope of PIARC 1995 equation while the intercept is almost ten times higher than the one in PIARC equation. Consequently, intercept loses its physical meaning of diameter of the spheres.

In the limit condition (very permeable hot mix asphalt), for the current thickness of the surface layer, the MTD can be ideally associated with a cylinder having the height which equals a fraction of the thickness of the layer (MTD=t*, where t*<t, and t=thickness of the friction layer).

In contrast, as for MPD, its maximum value (very porous asphalt concretes) depends on the nominal maximum aggregate size (NMAS, see also Henault et al., 2011 [58]).

Based on the above two models were set up.

The first model is below shown, where α, β, and χ are positive coefficients to calibrate:

$$MPD = \frac{\left(\frac{MTD}{0.8} - \frac{0.2}{0.8}\right)}{e^{\alpha \cdot MTD}} + \left(1 - e^{\beta \cdot (-MTD+0.2)}\right) \cdot \chi \cdot NMAS \quad (1)$$

Note that: i) when MTD tends to 0.2, then MPD tends to zero; ii) when MTD tends to increase, then MPD tends to a fraction of the NMAS.
More in general, the following equation can be written:

$$MPD = \frac{\left(\frac{(MTD - q)}{m}\right)}{e^{\alpha \cdot MTD}} + \left(1 - e^{\beta \cdot (-MTD+q)}\right) \cdot \chi \cdot NMAS \quad (2)$$

Where m and q, together with α, β, and χ are positive coefficients to calibrate.
The same concepts can be used to derive a different, simpler, second algorithm.
Indeed, based on the above, as far as low values of MTD and MPD are considered, the curve MPD(MTD) needs to satisfy the following conditions:

a) Low values dominion (see Figure 1, left). When close to the origin, the curve must have a first derivative (∂MPD/∂MTD) around 1/m (where m≅0.8, as *per* PIARC 1995 experiment see Wambold et al, 1995 [43]).
b) Low values dominion (see Figure 1, left). The curve must pass for the point MTD≅q, MPD≅0, where q≅0.2mm, as *per* PIARC 1995 experiment.
c) High values dominion (see Figure 1, right). the curve must have a first derivative close to zero, when it approaches (from left) the point MPD≅NMAS*, MTD≅t*, where NMAS* is a linear function of the nominal maximum aggregate size and t* is a linear function of the thickness t of the permeable layer.

Based on the above, in the case of a parabolic curve, the following equation can be derived:

$$MPD = -\frac{1}{2mt^*} \cdot MTD^2 + \frac{1}{m} \cdot MTD - \frac{q}{m} \quad (3)$$

Note that the above m and q refer to the well-known (PIARC, 1995) curve:

$$MTD = m \cdot MPD + q \quad (4)$$

Where m≅0.8 and q≅0.2mm.

Note that for regression purposes, the above equation can be simply rewritten as:

$$MPD = d \cdot MTD^2 + e \cdot MTD - f \quad (5)$$

Note that the above equations (3) and (4) are defined for values of MTD lower than t*.
Note that equation (3) can be considered as a reference equation. It derives from the modelling of the two extreme areas (low and high values, DGFCs, PACs, and PEMs) and permits to overcome the existence of a maximum for an abscissa lower than t* (equations 1-2). Indeed, based on the data available to date, the existence of such a maximum of the curve MPD(MTD), which is theoretically possible in equations 1-2, is not well-grounded on data analysis.

3.2 Model calibration

Table 1 illustrates the main characteristics of the data set used to analyse, calibrate and validate the model.

Table 1. Data used for calibrate and validate the model

Acronym of pavement surface		S1	S2	P1	P2	P3	D1	P4	D2
Type		**SMA**	**SMA**	**PEM**	**PEM**	**PAC**	**DGFC**	**PEM**	**DGFC**
Data from		**Survey** (*)	**Survey** (*)	**Survey** (*)	**Survey** (*)	**Flintsch et al, 2003 [34]**	**Survey** (*)	**Exp** (**)	**Exp** (**)
Type of analysis		**CAL**	**CAL**	**CAL**	**CAL**	**CAL**	**CAL**	**VAL**	**VAL**
Average MPD (mm)		**1.01**	**1.56**	**2.70**	**2.53**	**2.14**	**0.72**	**2.62**	**0.72**
Average MTD (mm)		**0.77**	**1.14**	**3.63**	**3.58**	**3.07**	**0.49**	**4.30**	**0.51**
NMAS (mm)		**8**	**14**	**15**	**15**	**12.5**	**10**	**15**	**10**
Aggregate gradation passing	5/NMAS mm (***)	**10%**	**66%**	**78%**	**75%**	**86**	**53**	**77**	**55**
	2/5 mm	**50**	**15**	**6**	**15**	**11**	**17**	**12**	**15**
	0.075/2 mm	**32**	**10**	**9**	**4**	**1**	**24**	**5.5**	**23**
	<0.075 mm	**8**	**9**	**7**	**6**	**1**	**6**	**6.5**	**7**
bitumen content (%)		**6**	**5.5**	**4.7**	**5.3**	**5.5**	**5.7**	**5.0**	**5.9**

Legend. NMAS: nominal maximum aggregate size (mm) derived from aggregate gradation as the dimension corresponding to one sieve size larger than the first sieve to retain more than 10 percent of the material.
DGFC: dense-graded friction course.
PAC: porous asphalt concrete.
PEM: porous European mixes;
SMA: Stone Mastic Asphalt.
MPD: mean profile depth (ISO 13473-1 [1] and ASTM E 1845 [2], mm);
MTD: mean texture depth (ASTM E 965 [3] and EN 13036-1 [4], mm).
(*): Surveys carried out in the past by the same authors.
(**): New experiments carried out in this study (see Figure 3).
(***): percentage passing the sieve NMAS and retained on 5mm sieve.
CAL: Calibration;
VAL: validation

Based on the calibration of the model (equation 5), the following results were obtained for the parameters d, e, f:

$d=-0.05\ mm^{-1}$; $e=0.78\ mm^{0}$; $f=0.43mm$; $R^2=0.94$, $p=0.000$.

Note that the parameter f, even if close to zero, is very different from the one which was theoretically predicted (-0.25, see equation 3). This implies that the above curve doesn't pass for the point MTD=0.2mm, MPD=0mm, which is not satisfactory from a theoretical standpoint, even if this fact has a negligible practical importance for real DGFCs.

The parameter e is very different from the one which was theoretically predicted (1.250, see equation 3). This value of the first derivative in the origin of the axes (very dense hot mix asphalts) is lower than 1.250 and this fact depends on the necessity to fit both open and dense-graded mixes with a so simple (second-order) polynomial.

Under the abovementioned hypotheses (first derivative approaches zero when MTD approaches t*), it comes that d=-e/(2t*) and then t*=7.1mm. If simple computations are carried out (MPD(t*)) , this means that the extreme configuration (i.e, for PACs, often termed porous asphalts) entails MPDs and MTDs which are around the 10-20% of the correspondent NMAS and thickness. This occurrence derives from the experiments and simulations carried out on a quite copious data set. It implies that the model takes into account the physical meaning of MTD (*versus* t, thickness of the wearing course) and MPD (*versus* NMAS, nominal maximum aggregate size), achieving a viable and reasonable compromise between simplicity, physical configuration and numerical fitting.

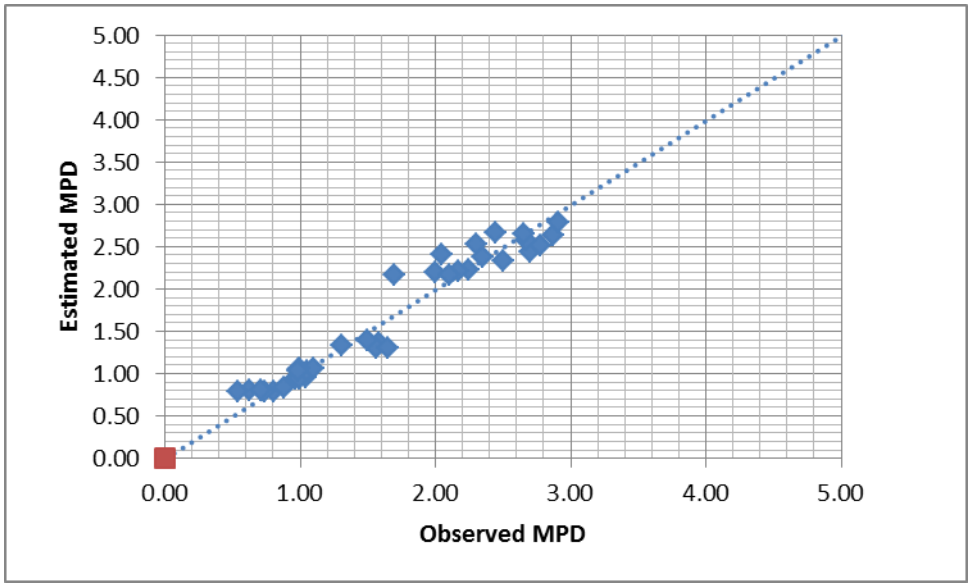

Figure 2. Observed (x-axis) versus estimated values of MPD

3.3 Experiments and Verification

An experimental plan was designed and carried out in the pursuit of obtaining new observations (data) for the dependent (MTD) and independent (MPD) variable (see Figures 3-7 and table 2). Experiments were carried out in Southern Italy (Figures 3 and 4). They were carried out as *per* the abovementioned standards for MPD (ISO 13473-1:1997 [1]) and sand patch texture (ASTM E965 [3]; EN 13036-1 [4]).

Two main types of wearing courses were investigated:

- dense-graded friction courses (D2) see Table 1 and Figure 3 (left);
- porous European mixes (P4), see Table 1 and Figure 3 (right).

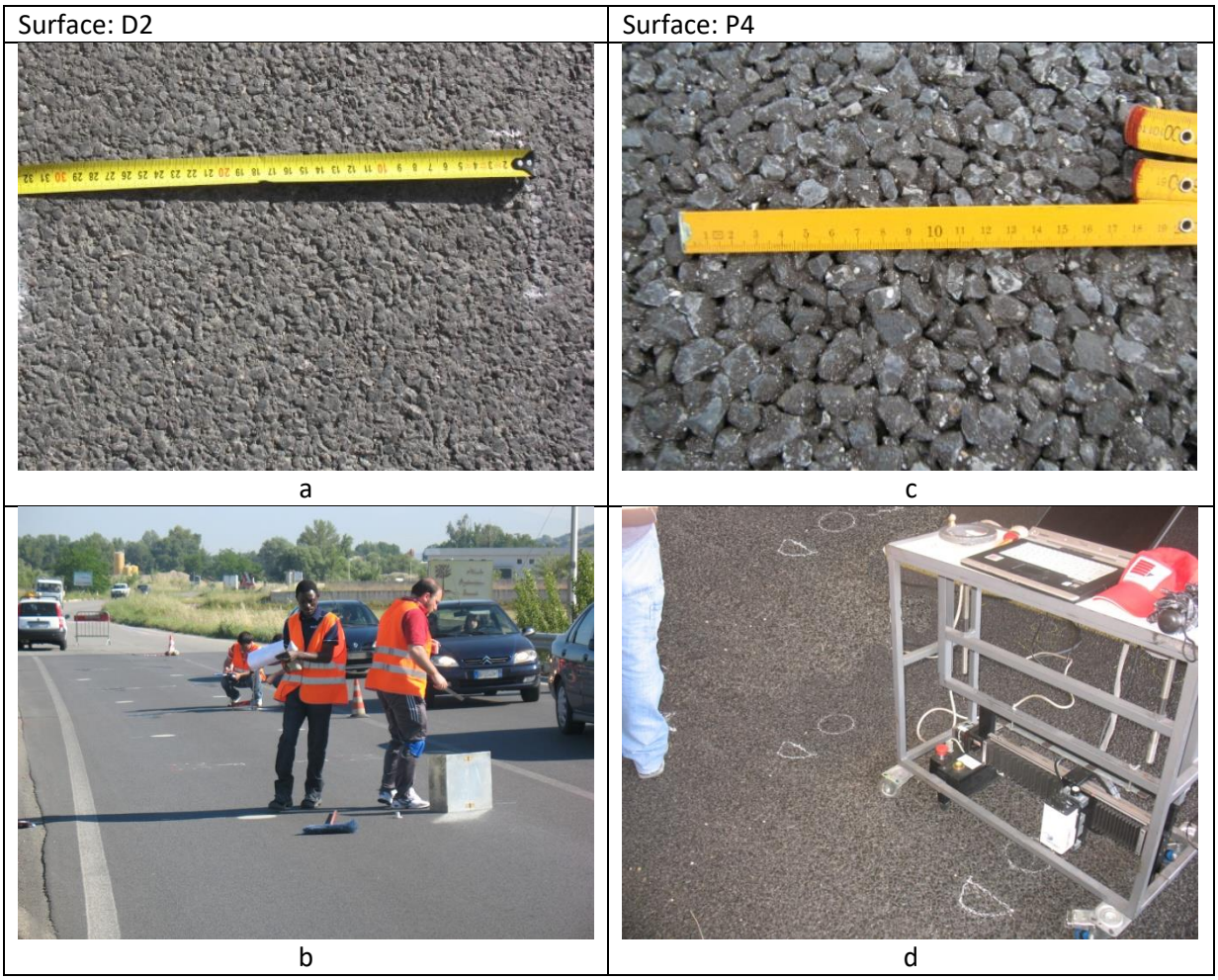

Figure 3. Experiments carried out. Left: friction course (D2, a and b). Right: PEM (P4, c and d)

In particular, laser profilometer scanning was carried out in terms of (x,z) coordinates, where z represents profile depths. A laser profilometer based on conoscopic holography was used (see Figure 4). The device has the following characteristics (ISO 13473-3 [60]): i) Mobility: Stationary, Slow (time on lane per single measurement equal or higher than 1 minute, according to ISO 13473-3 [6]); ii) Texture wavelength range: Range covered BD class 0.20÷50mm; iii) Pavement contact: Contactless devices; iv) Principle of operation: Laser profilometer; v) Obiective Focal Length: 100mm; vi) Max Vertical measuring range: 35mm; vii) Vertical resolution for class 0.003÷0.03 mm: 0.012mm; viii) Stand-off distance: 90mm; ix) Minimum horizontal resolution Δx (sampling interval) BD for class 0.05÷1 mm: 0.01mm; x) Angle coverage: 170° (Praticò et al., 2013 [12]).

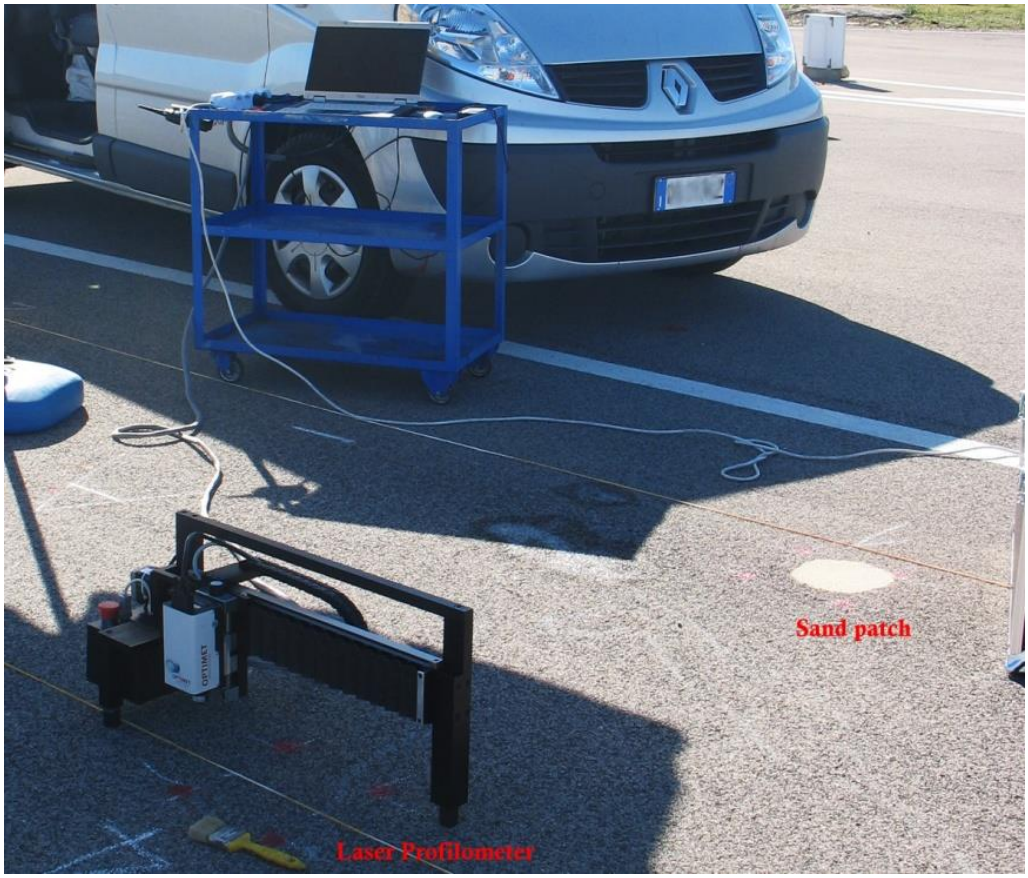

Figure 4. Sand patch (right) and laser (left) measurements for surface S2 (see table 1).

Model input-output transformations (input data versus macrotexture prediction) were compared to corresponding input-output transformations for the data derived through the new experiments, herein carried out.

Figure 5 and 6 illustrate how the curve formerly calibrated fits the new data.

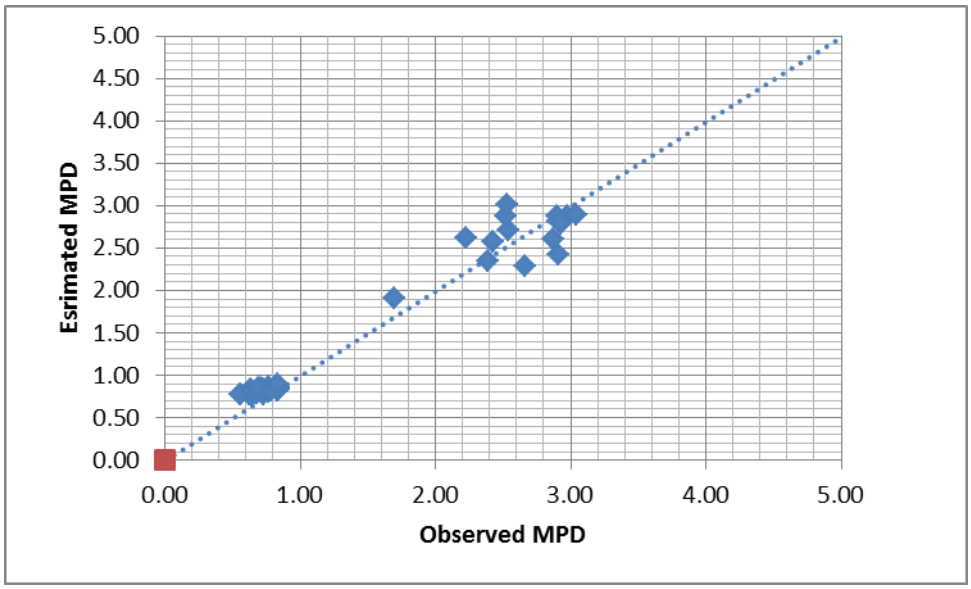

Figure 5. Observed versus estimated MPDs for the validation data set (see table 1).

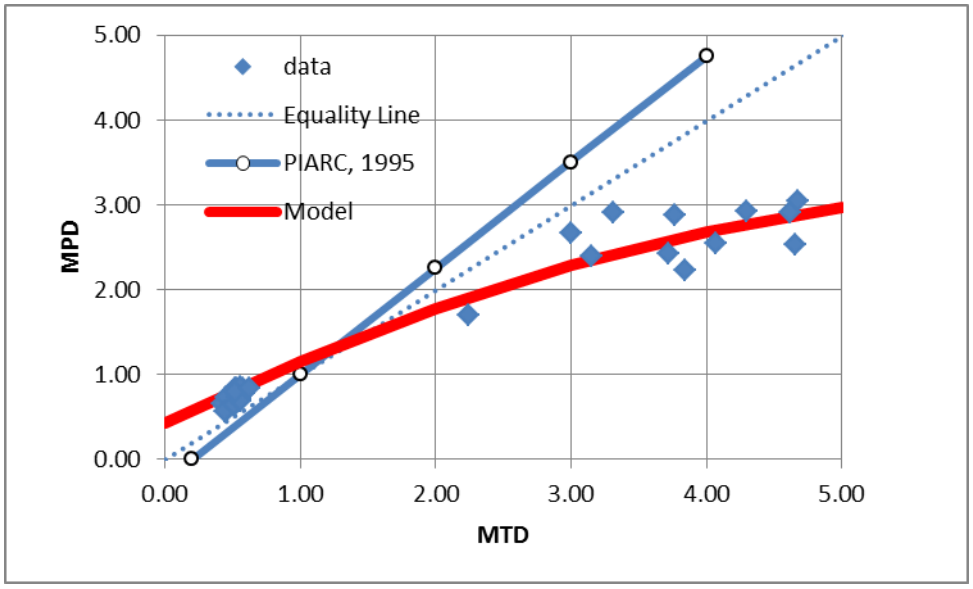

Figure 6. Validation data set and fitting curve (see table 1).

Table 2 and Figure 7 summarise experiments and analyses. They summarise all the data and information gathered in the literature and through the experiments and how obtained results related to them.

As for the three coefficients of the polynomial, note that d ranges from -0.11 to -0.05, e ranges from 0.75 to 1.25, and f ranges from -0.25 to 0.43. Importantly, these dominions are affected by the theoretical predictions more than by data fitting, being -0.11, 1.25 and -0.25 values obtained in the aim of obtaining a good consistency with PIARC, 1995 experiment (in which dense-graded mixes were used).

As for MPD and MTD averages (1.4-1.7mm versus 1.8-2.0 mm) and standard deviations (0.7-0.9mm versus 1.3-2.1mm) they appear to be quite consistent and reasonable and able to assure a consistent process of model building, calibration and validation.

By referring to the significance of the correlations (four cases in Table 2), note that:

i) R^2 is the R-square value: the higher it is, the higher the significance is; 0.05 and 0.01 are the significance levels commonly used;
ii) N is the number of data used (sample size): the higher N, the higher is the significance;
iii) the p-value reported in table 2 represents the probability of making the “wrong decision”, i.e. a decision to reject the null hypothesis (the two variables are not correlated) when the null hypothesis is actually true (Type I error, or "false positive determination"). The smaller the p-value is, the more significant the result is said to be;
iv) being $p<0.01$, it is confirmed that the correlations are significant at a 1% level of significance.

340 *Table 2. Summary of experiments and analysis*

	Unit	Overall	Calibration	Validation	Simplified model
d	mm^{-1}	-0.05	-0.05	-0.05	-0.109
e	-	0.76	0.78	0.78	1.250
f	mm	0.39	0.43	0.43	-0.250
R^2	-	0.95	0.94	0.96	0.93
N	-	76	35	40	76
t* derived	mm	7.2	7.1	7.1	5.7
Average MPD	mm	1.5	1.7	1.4	1.5
Standard deviation of MPD	mm	0.9	0.7	0.9	0.9
Average MTD	mm	1.9	2.0	1.8	1.9
Standard deviation of MTD	mm	1.8	1.3	2.1	1.8
Significance (p-value)	-	8.9E-51	6.3E-23	6.6E-30	3.35E-44

Legend. Overall: results obtained using all the data in Table 1. Calibration: results obtained using calibration data in Table 1. Validation: results obtained using validation data in Table 1. Simplified model: equation 3. d, e, f: coefficients in equation 5. R^2: coefficient of determination (indicates how well data fit the model); N: number of data used. t*: fraction of the thickness obtaining from $2dt^*+e=0$. Average MPD, MTD, Standard deviation of MPD, MTD: position and dispersion characteristics of the data set in Table 1. Significance: p-value, which is the probability of observing the effect given that the null hypothesis is true (results have occurred by chance alone). If $p<0.05$, then the result is statistically significant.

341

342 Figure7 shows the impact of parameters adjustment on the second-order polynomial.

343 It is important to observe that the simplified model in Table 2 and Figure 7 refers to the polynomial
344 based on PIARC 1995 (Wambold et al. 1995 [43]) straight line (MTD=q+m·MPD, with m=0.8;
345 q=0.2; e=m=1/0.8; f=q=-0.2/0.8), and was set up in order to carry out comparative analyses,
346 considering both PIARC 1995 straight line (MTD=0.2+0.8MPD) and purely statistical studies.

347 To this end, in Figure 7, the following twelve curves are considered: i) equality line; ii and iii)
348 polynomials based on the lowest (L) and highest (H) m and q in the literature (based on equation 4,
349 in this case no optimization was carried out; see curves L and H); iv) simplified model as *per*
350 equation 3; v) polynomials in which the adjustable parameters d, e, f were adjusted in order to
351 "best" fit the data through the least squares method (d, e, f "free", see equation 5); vi) polynomials
352 in which the adjustable parameter d was set free and remaining parameters were fixed based on
353 PIARC 1995 (Wambold et al. 1995 [43]) straight line (i.e., e=1/0.8; f=0.2/0.8); vii) e free (and
354 remaining parameters constrained, based on PIARC 1995); viii) f free (and remaining fixed based
355 on PIARC 1995); ix) d & e free (and remaining fixed based on PIARC 1995); x) d & f free (and
356 remaining fixed based on PIARC 1995); xi) d & e free (and remaining fixed based on PIARC 1995);
357 xii) PIARC 1995 straight line.

358 In summarising in Figure 7 there are two types of curves: four reference curves (Curves H, L,
359 Equality line, PIARC 1995) and eight curves derived in this paper (the remaining ones).

360 Results in Figure 7 confirm that all the above (seven) solutions (each one obtained by adjusting the
361 parameters of equation 5 to best fit the same data set) resulted in curves close to the case

362 "Simplified model" (equation 3). This fact means that the new algorithm has a good level of
363 consistency with the previous literature and extends to the dominion of innovative and more open
364 mixes the relationship between volumetric-based and laser-based indicators.

365

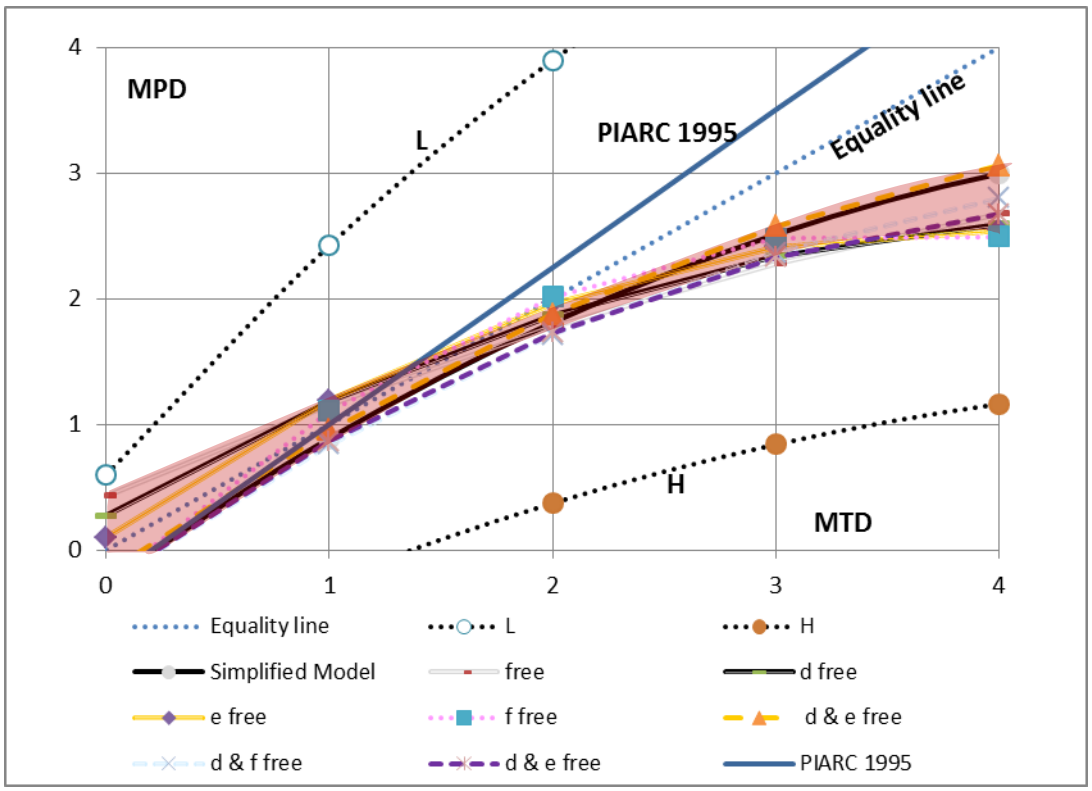

366
367 *Figure7. Impact of parameters adjustment on the second-order polynomial*

368 ## 4.Conclusions

369 It is well known that pavement texture impacts surface performance, tyre-vehicle interaction and
370 road safety.

371

372 Texture in the range of wavelengths between 0.5 and 50mm is termed macrotexture and can be
373 assessed in terms of MPD (2D derivation, based on ISO 13473-1 [1] and ASTM E 1845 [2]) and
374 MTD (3D – derivation, based on ASTM E965 [3] or EN 13036-1 [4]).

375 Based on the model set up and on the experiments and studies carried out it is possible to
376 conclude that:

377 • There is an evident divergence from linearity when open-graded mixtures are
378 considered. MPD and sand patch texture measure different properties and linear
379 correlations seem not to represent effectively this complexity and dissimilarity.
380 • There is a reasonable consistency of the majority of the studies conducted in the past
381 when only DGFCs are considered.
382 • The divergence between laser-based and volumetric-based macrotexture indicators
383 (when open-graded wearing courses are considered) has quite simple explanations and
384 physical reasons. It originates from the fact that the laser works in a two-dimensional

scenario, while the sand patch method has rational behind which is three-dimensional and more complex.

- A generalised and simple model has been set up and validated. It fits the data of a wide spectrum of wearing course types without neglecting the fundamental achievements which refer to the curves derived in the past.

Future research will focus on the following main issues: a) considering other advanced materials such as Porous Elastic Road Surfaces, which imply higher values of air voids content and surface macrotexture; b) considering other types of wearing courses in the area of intermediate macrotexture (bituminous surface treatments, etc.); c) investigating in more detail the possible relationship between the overall model (MPD versus MTD) and the advanced modelling of granular flows and water flows.
Further investigations will be also needed in the area close to the origin of the axes (ideally compact HMAs, very low values of MTD and MPD), where procedures and equipment precision can greatly affect the studies.
It is supposed that results outcomes of this research can benefit both researchers and practitioners.

References

[1] ISO 13473-1:1997. Characterization of Pavement Texture by Use of Surface Profiles. Part 1: Determination of Mean Profile Depth.
[2] ASTM E1845–01. Standard Practice for Calculating Pavement Macrotexture Mean Profile Depth. Vol. 04.03
[3] ASTM E965-96. Standard Test Method for Measuring Pavement Macrotexture Depth Using a Volumetric Technique. Vol. 04.03
[4] EN 13036-1. Road and airfield surface characteristics — Test methods — Part 1: Measurement of pavement surface macrotexture depth using a volumetric patch technique.
[5] Noyce D.A., Bahia H.U., Yambó J.M. and Kim G. (2005). Incorporating road safety into pavement management:Maximizing asphalt pavement surface friction for road safety improvements. DRAFT Literature Review & State Surveys, Midwest Regional University Transportation Center Traffic Operations and Safety (TOPS) Laboratory.
[6] Freitas E. and P. Pereira, M. L. Antunes and P. Domingos (2008), Analysis of Test Methods for Texture Depth Evaluation Applied in Portugal. C-TAC - Comunicações a Conferências Nacionais.
[7] NCHRP 291, 2000. Evaluation of Pavement Friction Characteristics. NCHRP Synthesis 291, Transportation Research Board, Washington DC.
[8] Do, M.-T., Marsac, P., Delanne, Y.,2004. Prediction of Tyre/wet Road Friction from Road Surface Microtexture and Tyre Rubber Properties. 5th Symposium on Pavement Surface Characteristics-Roads and Airports, World Road Association, Toronto, Canada.
[9] Kim H.B., Lee S.W., Hyun T.J. and Lee K.H. (2013). Measurement of Texture Depth of Pavement Using Potable Laser Profiler. Proceedings of the Eastern Asia Society for Transportation Studies, Vol.9.
[10] SILVIA, 2006. Guidance Manual for the Implementation of Low-Noise Road Surfaces. FEHRL Report 2006/02, Forum of European National Highway Research Laboratories, Brussels, Belgium.
[11] Lu Q. and Harvey J.T. (2011). Laboratory evaluation of open-graded asphalt mixes with small aggregates and various binders and additives. Transportation Research Board 90th Annual Meeting, Washington D.C., USA, 61-69.
[12] Praticò, F.G., Vaiana, R., Iuele T. (2013). Acoustic absorption and surface texture: An experimental investigation. INTER-NOISE 2013, the 42nd International Congress and Exposition on Noise Control Engineering, Innsbruck, Austria, 15-18 September 2013. ISBN: 978-163266267-5.
[13] Praticò, F.G., Vaiana, R., Fedele R. (2014). A study on the dependence of PEMs acoustic properties on incidence angle. International Journal of Pavement Engineering DOI:10.1080/10298436.2014.943215
[14] Delanne, Y. and Daburon, P., 1999. Unevenness and Vibrational Comfort of light Cars. International Symposium of the Environmental Impact of Road Unevenness, Oporto, Portugal.
[15] Bendtsen H. (2004). Rolling resistance, fuel consumption. A literature review. Road Directorate, Danish Road Institute, ISSN: 1395-5530.

[16] Sohaney R.C. and Rasmussen R. O., (2013). Pavement Texture Evaluation and Relationships to Rolling Resistance at MnROAD. Minnesota Department of Transportation, Research Services. Final Report: MN/RC 2013-16. *Available from*: http://www.dot.state.mn.us/research/TS/2013/201316.pdf
[17] Nordströdm O. and Andersson O., (1996). Chapter 11. Modelling Tyre Consumption. Swedish Research on Tyre Consumption, Book.
[18] Domenichini, L. and Martinelli, F., 2004. Influence of the Road Characteristics on Tyre Wear. 5th Symposium on Pavement Surface Characteristics-Roads and Airports, World Road Association, Toronto, Canada.
[19] China S. and James D.E (2012). Influence of pavement macrotexture on PM10 emissions from paved roads: A controlled study. Atmospheric Environment, Volume 63, 2012, Pages 313-326. doi:10.1016/j.atmosenv.2012.09.018
[20] Amato F., Pandolfi M., Alastuey A., Lozano A., Contreras González J., Querol X., (2013). Impact of traffic intensity and pavement aggregate size on road dust particles loading". Atmospheric Environment, Volume 77, 2013, Pages 711-717. doi:10.1016/j.atmosenv.2013.05.020
[21] Wang, T., Harvey, J., Kendall, A., (2014). Reducing greenhouse gas emissions through strategic management of highway pavement roughness, Environ. Res. Lett. 9, 034007 (10pp) doi:10.1088/1748-9326/9/3/034007.
[22] Boscaino G. and Praticò F. G., (2001). Classification et inventaire des indicateurs de la texture superficielle des revêtements des chausses. Bulletin des Laboratories des Pontes et Chausses, 234, 17–34. ISSN: 1269-1496
[23] Abe, H., Tamai, A., Henry, J. and Wambold. J., 2001. Measurement of Pavement Macrotexture With Circular Texture Meter. Transportation Research Record 1764, pp 201- 209, Transportation Research Board, Washington DC.
[24] Aktaş B., Gransberg D.D., Riemer C. and Pittenger D. (2011). Comparative Analysis of Macrotexture Measurement Tests for Pavement Preservation Treatments. Transportation Research Record, 2209, 34-40.
[25] Blanchard C. and Holloway (2013). Road Surface Texture Measurement Recommended Investigatory Levels. Technical Note n. 25, Department of planning transport and infrastructure, Government of South Australia.
[26] China S. and James D.E. (2012). Comparison of Laser-Based and Sand Patch Measurements of Pavement Surface Macrotexture. Journal of transportation engineering © ASCE, 138, 176-181.
[27] Sengoz B., Topal A., Tanyel S. (2012). Comparison of pavement surface texture determination by sand patch test and 3D laser scanning. Periodica Polytechnica Civil Engineering, Vol:56, No:1, pp:73-78, 2012.
[28] ASTM STP583. Surface Texture Versus Skidding: Measurements, Frictional Aspects, and Safety Features of Tire-Pavement Interactions.
[29] Cooley Jr. L. A. (1999). Permeability of superpave mixtures: evaluation of field permeameters. NCAT Report 99-01
[30] Yaacob,H., Hassan, N.A., Hainin,M.R., Rosli, M.F., (2014). Comparison of Sand Patch Test and Multi Laser Profiler in Pavement Surface Measurement. Jurnal Teknologi, Volume 70,N. 4, 2014. DOI: http://dx.doi.org/10.11113/jt.v70.3497.
[31] Rodriguez, P.P.C., Dominguez, F.S., García, J.A.R., (2014). Measurement Of Surface Macrotexture On Runways Of Airports. Texturometers Laser Versus Traditional Methods Of Measurement. FAA Worldwide Airport Technology Transfer Conference, Galloway, New Jersey, USA.
[32] Stroup-Gardiner M. and Brown E.R. (2000). Segregation in Hot-Mix Asphalt Pavements. National Cooperative Highway Research Program (NCHRP) Report 411, Transportation Research Board (TBR), Auburn University (USA).
[33] Davis R.M. (2001). Comparison of Surface Characteristics of Hot-Mix Asphalt Pavement Surfaces at the Virginia Smart Road. Thesis Submitted to the Faculty of Virginia Polytechnic Institute and State University In partial fulfilment of the requirements for the degree of: Master of Science In Civil and Environmental Engineering, Blacksburg, Virginia.
[34] Flintsch G.W., McGhee K.K. and De León Izeppi E. (2003). Using high-speed texture measurements to improve the uniformity of hot-mix asphalt. Virginia Transportation Research Council (VTRC) 03-R12.
[35] Hanson D. I. and Prowell B.D. (2004). Evaluation of circular texture meter for measuring surface texture of pavements. National Center for Asphalt Technology Report 04-05, Auburn University.
[36] Sullivan B.W. (2005). Development of a fundamental skid resistance asphalt mix design procedure. Proceedings, International Conference on surface friction, Christchurch, New Zeland.
[37] Goodman S.N., Hassan Y. and Halim A.O.A.E. (2006). Preliminary Estimation of Asphalt Pavement Frictional Properties from Superpave Gyratory Specimens and Mix Parameters. Transportation Research Board (TBR) 2006 Annual Meeting Proceedings on CD-Rom.

[38] Praticò F.G. et al., 2010. HMA composition versus surface characteristics: issues and perspectives to optimise road asset management. In: Proceedings of 2nd international conference on transport infrastructures, 4–6 August 2010. São Paulo, Brazil. Guimarães: Universidade do Minho Escola de Engenharia, 549–561.
[39] D'Apuzzo M., Evangelisti A., Nicolosi V. (2012). Preliminary findings for a prediction model of road surface macrotexture. SIIV – 5th International Congress – Sustainability of road infrastructures. Procedia – Social and behavioral sciences 53 (2012), 1111 – 1120. DOI: 10.1016/j.sbspro.2012.09.960
[40] Henann, D., L., and Kamrin, K. (2013). A predictive, size-dependent continuum model for dense granular flows, PNAS, vol. 110 no. 17, David L. Henann, 6730–6735, doi: 10.1073/pnas.1219153110.
[41] Meegoda J.N., Rowe G.M., Hettiarachchi C.H., Bandara N. and Sharrock M.J. (2002).Correlation of Surface Texture, Segregation, and Measurement of Air Voids. FHWA-NJ-2002-026. Federal Highway Administration U.S. Department of Transportation, Washington, D.C.
[42] Vaiana R., Capiluppi G.F., Gallelli V., Iuele T. and Minani V. (2012). Pavement Surface Performances Evolution: an Experimental Application. SIIV - 5th International Congress - Sustainability of Road Infrastructures. Procedia - Social and Behavioral Sciences 53 (2012), 1151 – 1162.
[43] Wambold, J., Antle, C., Henry, J., Rado, Z., Descornet, G., Sandberg, U., Gothié, M. and Huschek, S., 1995. International PIARC Experiment to Compare and Harmonize Texture and Skid Resistance Measurement. Final report, No. 01.04.T, to the Technical Committee on Surface Characteristics, World Road Association (PIARC), Paris.
[44] Wang W., Yan X., Huang H., Chu X and Abdel-Aty M. (2011). Design and verification of a laser based device for pavement macrotexture measurement. Transportation Research Part C 19 (2011), 682–694.
[45] Losa, M., Leandri, P., Bacci, R. (2007). Measurements of pavement macrotexture with stationary and mobile profilometers, Fifth International Conference on Maintenance and Rehabilitation of Pavements and Technological Control (MAIREPAV5).
[46] De Fortier Smit A. and Waller B. (2007). Evaluation of the ultra-light inertial profiler (ULIP) for measuring surface texture of pavements. National Center for Asphalt Technology (NCAT) Report 07-01, Auburn University.
[47] Mackey G. (2005). Road Surface Friction: Measurement, Testing and Accuracy. International surface friction conference, Christchurch, New Zealand, 14P (SESSION 4)
[48] Flintsch G.W., De León E., McGhee K.K. and Al-Qadi I.L. (2007). Pavement Surface Macrotexture Measurement and Applications. Transportation Research Record, 1860, Paper No. 03-3436.
[49] Fisco N. and Sezen H. (2013). Comparison of surface macrotexture measurement Methods. Journal of Civil Engineering and Management, 19:sup1, 153-160
[50] Flintsch G.W., Al-Qadi I.L., Davis R. and McGhee K.K. (2002). Effect of HMA Properties on Pavement Surface Characteristics. Pavement Evaluation Conference, 2002, Roanoke, Virginia, USA.
[51] Xiao Y., Van de Ven M.F.C., Molenaar A.A.A., Wu S.P. and Verwaal W., (2011). Surface Texture of Antiskid Surface Layers Used on Runways. Transportation Research Board 2011 Annual Meeting.
[52] ASTM 2157-2005. Standard Test Method for Measuring Pavement Macrotexture Properties Using the Circular Track Meter
[53] Nicholls, J.C. (1997). Review of UK Porous Asphalt Trials. TRL Report 264
[54] Vilaça J.L., Fonseca J.C., Pinho A.C.M. and Freitas E. (2010). 3D surface profile equipment for the characterization of the pavement texture – TexScan. Mechatronics 20 (2010), 674–685.
[55] Praticò, F.G., Vaiana, R., (2013). Permeable friction courses: area-based vs. line-based surface performance and indicators. INTER-NOISE 2013, the 42nd International Congress and Exposition on Noise Control Engineering, Innsbruck, Austria, 15-18 September. ISBN: 978-163266267-5.
[56] Prowell, B.D., and D.I. Hanson. (2005). Evaluation of Circular Texture Meter for Measuring Surface Texture of Pavements. In Transportation Research Record No. 1929, TRB, National Research Council, Washington, D.C., 2005, pp. 88-96.)
[57] Freitas, E., Freitas, C., & Bragab, A.C., (2014). The analysis of variability of pavement indicators: MPD, SMTD and IRI. A case study of Portugal roads. International Journal of Pavement Engineering, Volume 15, Issue 4, pages 361-371, DOI:10.1080/10298436.2013.807343.
[58] Henault J.W., Bliven P.E. and J. Bliven (2011). Characterizing the Macrotexture of Asphalt Pavement Designs in Connecticut. Research Project: SPR-2243 Report 2. Report No. CT-2243-2-10-3.

559 [59] Roberts, F.L., Kandhal, P.S., Brown, E.R., Lee, D.Y., and Kennedy, T.W. (1996). Hot Mix Asphalt
560 Materials, Mixture Design, and Construction. National Asphalt Paving Association Education
561 Foundation. Lanham, MD.
562 [60] ISO 13473-3:2002. Characterization of pavement texture by use of surface profiles. Part3:
563 specifications and classification of profilometers.